Effect of van der Waals Interactions on the Raman Modes in Single Walled Carbon Nanotubes

A. M. Rao,[1,*] J. Chen,[2,†] E. Richter,[2] U. Schlecht,[1] P. C. Eklund,[3] R. C. Haddon,[2] U. D. Venkateswaran,[4] Y.-K. Kwon,[5,‡] and D. Tománek[5]

[1]*Department of Physics and Astronomy, Clemson University, Clemson, South Carolina 29634*
[2]*Department of Chemistry, University of Kentucky, Lexington, Kentucky 40506*
[3]*Department of Physics, Pennsylvania State University, University Park, Pennsylvania 16802*
[4]*Department of Physics, Oakland University, Rochester, Michigan 48309*
[5]*Department of Physics and Astronomy and Center for Fundamental Materials Research, Michigan State University, East Lansing, Michigan 48824*

(Received 26 July 2000)

We have measured the Raman spectrum of individual single walled carbon nanotubes in solution and compare it to that obtained from the same starting material where the tubes are present in ordered bundles or ropes. Interestingly, the radial mode frequencies for the tubes in solution are found to be $\sim 10\ \mathrm{cm}^{-1}$ higher than those observed for tubes in a rope, in apparent contradiction to lattice dynamics predictions. We suggest that there is no such contradiction, and propose that the upshift is due rather to a decreased energy spacing of the Van Hove singularities in isolated tubes over the spacings in a rope, thereby allowing the same laser excitation to excite different diameter tubes in these two samples.

DOI: 10.1103/PhysRevLett.86.3895 PACS numbers: 78.30.Na

The dominant experimental technique for studying phonons in single walled carbon nanotubes (SWNTs) has been Raman spectroscopy [1–5]. Until now, almost all Raman spectra have been collected on nanotube bundles that are synthesized by the pulsed laser vaporization (PLV) [6] or the electric arc (EA) [7] methods. These bundles contain on the order of 100 well-aligned SWNTs arranged in an approximately closed-packed triangular lattice. A typical Raman spectrum of the EA-derived SWNT bundles obtained using the 1064 nm excitation wavelength exhibits two prominent features at $\omega_R \sim 160\ \mathrm{cm}^{-1}$ (radial band) and $\omega_T \sim 1590\ \mathrm{cm}^{-1}$ (tangential band). The position and the line shape of these bands have been used extensively to determine the SWNT diameter distribution and semiconducting/metallic nature of SWNTs.

The tube-tube interactions within SWNT bundles are weak, similar to the coupling between adjacent graphene planes in 3D crystalline graphite or the interball coupling found in solid C_{60}. This weak intertube coupling is dominated by the van der Waals interaction, but contains a nonzero covalent component that has been shown theoretically and experimentally to have significant influence on the vibrational [8–12] and electronic states for carbon nanotubes [13–15]. Recently, Chen *et al.* [5] reported the synthesis of soluble shortened and full-length single walled carbon nanotubes. Details of the preparation and characterization of the solubilized tubes (S-SWNTs) are described elsewhere [5]. Atomic force microscope images showed that the majority of the bundled SWNTs were separated into small bundles (2–5 nm in diameter) and isolated tubes during the solubilization process [5].

In Fig. 1, the Raman spectrum of S-SWNTs in CS_2 is compared to that obtained for bundled SWNTs, the latter in powder form. The S-SWNTs and bundled SWNTs referred to in Fig. 1 stem from the same as-prepared EA material. Three modes, previously identified with A_{1g}, E_{1g}, and E_{2g} symmetries and frequencies that are nearly independent of the tube diameter, are expected near the 1590 cm^{-1} band for achiral tubes [1]. For the chiral tubes, six modes are Raman active with A_1, E_1, and E_2 symmetries [16]. In contrast to the high frequency band at 1590 cm^{-1}, the low frequency band centered $\sim 160\ \mathrm{cm}^{-1}$ is identified with A_{1g}

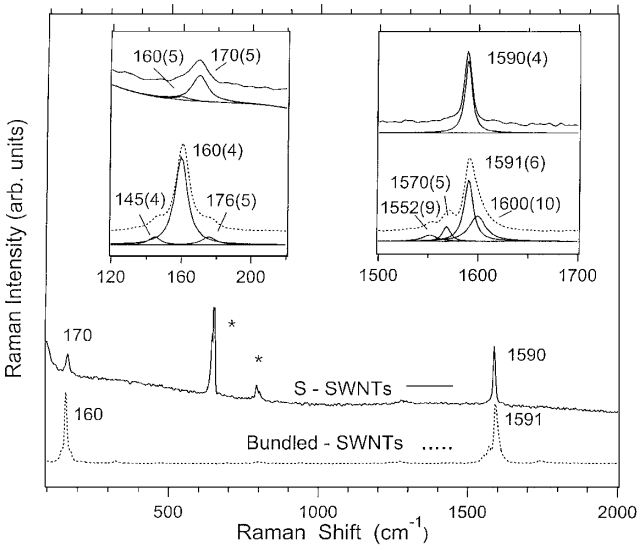

FIG. 1. Room temperature Raman spectrum of arc synthesized bundled SWNTs and solubilized SWNTs (S-SWNTs) in CS_2 (excitation wavelength = 1064 nm). The peaks identified by * are attributed to CS_2. The tangential band intensity is set to a constant peak intensity value so that the radial band intensities in the two spectra can be compared. Left- and right-hand insets show, respectively, the deconvolution of the radial and tangential bands in bundled and S-SWNTs. The vertical and horizontal axes for the two insets correspond, respectively, to the Raman intensity and shift. The numbers within parentheses refer to the full width at half maximum intensity of the Raman lines.

radial breathing modes whose frequency is strongly dependent on the tube diameter [16]. Consistent with the calculated mode frequencies and intensities, other weak Raman-active features have been observed in the intermediate phonon frequency region between ω_R and ω_T [1].

For an isolated SWNT, theoretical calculations have shown that the radial mode frequency ω_R' exhibits a particularly simple dependence on the tube diameter d' as [3]

$$\omega_R' \sim 224\ \mathrm{cm}^{-1} \cdot \mathrm{nm}/d'. \quad (1)$$

(Henceforth, primed and unprimed notation correspond, respectively, to isolated and bundled SWNTs.) Equation (1) has been widely used to determine the tube diameter distribution in samples containing both isolated and bundled nanotubes, since Raman spectroscopy provides a quick and convenient technique for sample characterization. Thus, care has to be taken to understand the origin of potential deviations from this relationship. As mentioned above, most Raman spectra have been obtained for bundled nanotubes. Because of the space restrictions imposed by the presence of neighboring tubes, tube-tube interactions within a bundle have been predicted to cause a $\sim$6–20 cm^{-1} up-shift in ω_R with respect to the corresponding value in isolated tubes, depending on particular theoretical calculations [8,9,11,15]. The effect of intertube interactions on the vibrational modes of SWNTs was first reported by Venkateswaran *et al.* [8] and has been used to interpret shifts in both ω_R and ω_T that were induced by applying external pressure. Comparing these experimental results to those obtained from a generalized tight binding calculation, which included the effects of the externally applied pressure, the simple $\omega_R' \sim 224\ \mathrm{cm}^{-1} \cdot \mathrm{nm}/d'$ relation for isolated tubes was generalized to nanotubes inside a bundle by the addition of a nearly constant upshift of $\sim$7% for tubes in the diameter range $0.7\ \mathrm{nm} < d < 1.5\ \mathrm{nm}$ [8,9]. Thus, in the case of bundled SWNTs, Eq. (1) is modified as

$$\omega_R \sim (224\ \mathrm{cm}^{-1} \cdot \mathrm{nm}/d) + \Delta\omega_R\,, \quad (2)$$

where $\Delta\omega_R$ is the anticipated up-shift due to tube-tube interactions which is approximately independent of the tube diameter in the restricted range of diameters.

According to Eq. (2), the observed up-shift in ω_R from bundled to S-SWNTs in Fig. 1 is anomalous, since the loss of intertube forces in S-SWNTs would be expected to soften ω_R relative to its frequency of 160 cm^{-1} observed in the Raman spectrum of bundled SWNTs. It should be noted that shifts in ω_R or ω_T have also been observed in doped nanotube bundles, where they have been related to the charge transfer between the nanotubes and the alkali metal (down-shift) or halogen dopants (up-shift) [17]. However, unlike the tube-tube coupling which affects mainly ω_R and not ω_T (see, for example, Fig. 1), charge transfer induced by doping was found to affect *both* the radial and the tangential mode frequencies to a large extent [17]. Clearly, for the spectra depicted in Fig. 1, the 10 cm^{-1} up-shift in ω_R upon forming S-SWNTs from bundled SWNTs cannot be attributed to charge transfer, since ω_T for S-SWNT exhibits an insignificant frequency shift from the value observed in bundled SWNTs.

It is also of interest to note from the right-hand inset of Fig. 1 that the loss of intertube interactions in the S-SWNTs in CS_2 leads to narrower linewidths for the tangential band relative to those observed in bundled SWNTs. A Lorenztian line shape analysis reveals at least four narrow subbands for the bundled SWNTs and a single narrow mode for S-SWNTs in CS_2. Similarly, from the left-hand inset in Fig. 1 for the radial band, a reduced number of Lorentzians is observed in the spectrum of S-SWNT sample when compared to that of the bundled SWNTs. It is not yet understood how tube-tube interactions might affect the number of tangential bands observed.

In Fig. 2, we compare the radial and tangential bands of PLV synthesized bundled SWNTs and *solid* full length PLV synthesized S-SWNTs (i.e., solubilized full length SWNTs obtained by evaporating the organic solvents). Unfortunately, the Raman spectra of S-SWNT dissolved in organic solvents (CS_2 or THF) obtained using visible laser excitations showed strong luminescence, and prevented us from detecting the radial or the tangential bands. The origin of this luminescence is not understood at present and warrants an independent study. The radial bands in solid S-SWNTs are consistently up-shifted relative to those of bundle SWNTs in all spectra depicted in Fig. 2(a). On the other hand, narrowing of the tangential band in S-SWNTs in CS_2 (see right-hand inset of Fig. 1) is absent in the tangential bands in solid S-SWNTs [Fig. 2(b)]. At least two important conclusions can be drawn from the Raman data presented in Figs. 2(a) and 2(b):

(i) Both semiconducting and metallic tubes exhibit $\sim$10 cm^{-1} up-shift as bundled tubes are solubilized. As Pimenta *et al.* [18] have argued, the 647.1 nm excitation couples predominantly to metallic tubes in the sample.

(ii) The relatively broader tangential band in solid S-SWNTs compared to that of S-SWNT in CS_2 suggests that the organic solvent-nanotube interactions have a smaller influence on the tangential mode lifetime than the tube-tube interactions in solid S-SWNTs.

Of particular importance to the discussion of the anomalous up-shift in ω_R is the electronic density of states (DOS) of isolated and bundled nanotubes with a diameter distribution representative of the sample. For the sake of simple comparison, we restrict our discussion to (8,8)–(11,11) armchair tubes, although similar calculations can be performed for zigzag and chiral tubes. A density functional formalism within the local density approximation (LDA) was used [14]. The tight-binding parametrization, based on LDA electronic structure results [19], had been used successfully to describe the effect of intertube coupling on quantum transport [20] and the opening of pseudogaps in bundled and multiwalled nanotubes [14,21]. The calculated electronic DOS of these quasi-1D systems, presented

in Fig. 3, shows sharp singularities at energies E_i, associated with the $(E - E_i)^{-1/2}$ Van Hove singularities. The electronic DOS plots show that the metallic tubes have a small, nearly constant DOS near the Fermi level (E_F). Our results indicate that intertube coupling causes an additional band dispersion of ~0.2 eV, which not only opens up a pseudogap at E_F but also broadens by the same amount the Van Hove singularities and the peak positions shift away from E_F. This leads to a net increase of the energy spacing Δ_1 between the first, and Δ_2 between the second, pair of Van Hove singularities in the electronic DOS for bundled nanotubes (Table I).

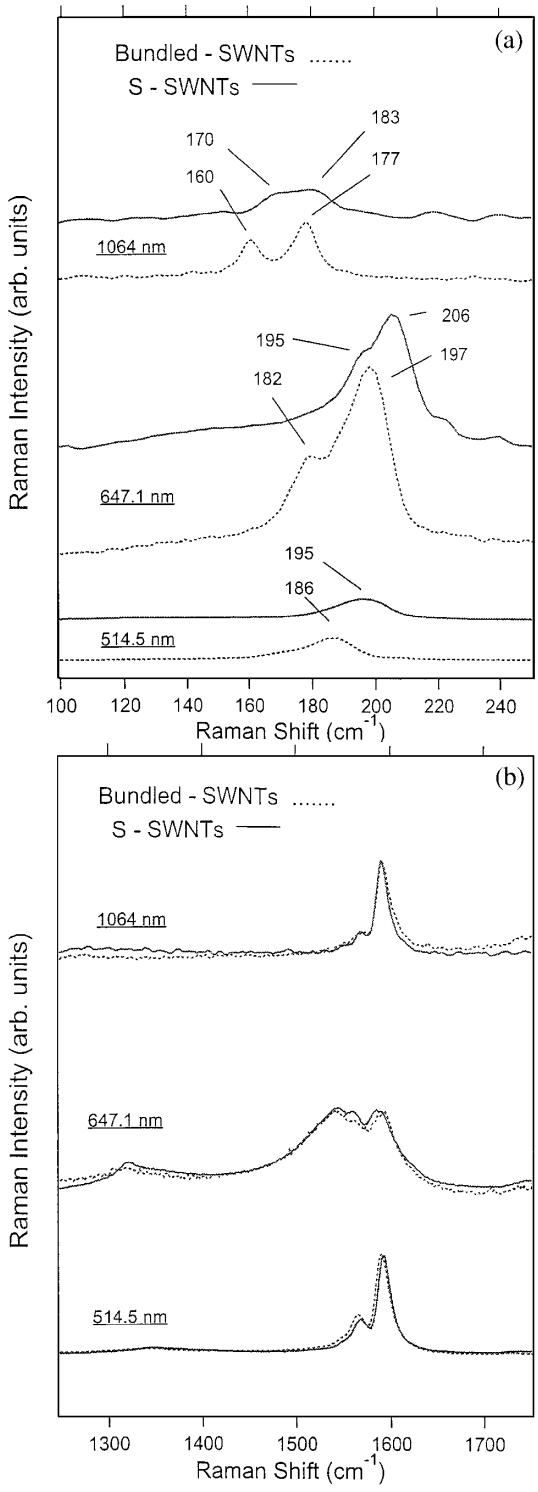

FIG. 2. Comparison of the radial (a) and tangential bands (b) in the PLV synthesized bundled and S-SWNTs for three laser excitation energies. In (b), the tangential bands for the bundled and S-SWNTs are superimposed for comparison of the linewidths.

Quantum confinement effects were observed in the Raman spectra of SWNT bundles through the resonant Raman enhancement effect between the excitation laser energy (E_{laser}) and the electronic transitions between the Van Hove singularities in the quasi-1D DOS in the valence and conduction bands of carbon nanotubes [1]. The combined scanning tunneling spectroscopy studies on PLV synthesized SWNTs [22,23] and optical transmission spectra taken from SWNTs synthesized using Ni:Y catalyst in the EA method [24] yield the approximate relations for semiconducting and metallic nanotubes, respectively:

$$\Delta_1' = \alpha/d'. \tag{3a}$$

In the above relation between Δ_1' and the tube diameter d', tight-binding theory shows that $\alpha = 2\gamma_0 d_{\text{C-C}}$ for semiconducting tubes and $\alpha = 6\gamma_0 d_{\text{C-C}}$ in metallic tubes, where γ_0 is the nearest neighbor overlap energy (or the transfer integral of a tight-binding model) and $d_{\text{C-C}}$ is the nearest neighbor distance in the hexagonal network. Amending this equation for intertube interactions, we have

$$\Delta_1 = \alpha/d + \delta\Delta_1\,. \tag{3b}$$

We now discuss the origin of the anomalous up-shift in ω_R in the Raman spectrum for S-SWNTs. The

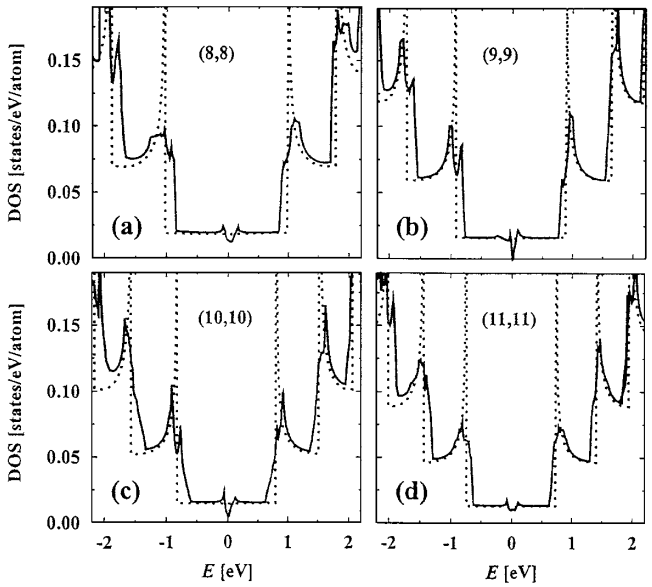

FIG. 3. Density of states of isolated (dotted lines) and bundled (solid lines) (8,8) (a), (9,9) (b), (10,10) (c), and (11,11) (d) carbon nanotubes. Clearly visible is the appearance of the pseudogap near $E_F = 0$ and the broadening of the Van Hove singularities, as isolated nanotubes bundle up into a close-packed triangular lattice. The tube indices (n, n) refer to armchair tubes (Ref. [16]).

TABLE I. Calculated energy difference, Δ_1, between the first and, Δ_2, between the second pairs of Van Hove singularities in the electronic density of states for isolated tubes and weakly interacting tubes in a bundle. The difference between the tube and bundle values is denoted by $\delta\Delta$. All energy values are in eV units.

(n, n)	Δ_1 (tube)	Δ_1 (rope)	$\delta\Delta_1$	Δ_2 (tube)	Δ_2 (rope)	$\delta\Delta_2$
(8,8)	2.03	2.23	0.20	3.69	3.89	0.20
(9,9)	1.83	1.99	0.16	3.39	3.55	0.16
(10,10)	1.64	1.84	0.20	3.12	3.29	0.17
(11,11)	1.49	1.63	0.14	2.87	2.98	0.11

$\sim 10\ \mathrm{cm}^{-1}$ up-shift can be understood and estimated numerically via Eqs. (1)–(3). Using the calculated value for $\Delta\omega_R \sim 14\ \mathrm{cm}^{-1}$ in bundled tubes in Ref. [9], Eq. (2) can be rewritten as

$$\omega_R \sim 224\ \mathrm{cm}^{-1} \cdot \mathrm{nm}/d + 14\ \mathrm{cm}^{-1}. \quad (4)$$

Because of the resonant Raman scattering process in SWNTs, at a fixed excitation laser energy ($E_{\mathrm{laser}} = \Delta_1$), it follows from Eqs. (3a) and (3b) that the following equality should be satisfied as the bundles are processed into isolated tubes:

$$\alpha/d' = \alpha/d + 0.2\ \mathrm{eV}. \quad (5)$$

For $\gamma_0 \sim 2.9$ eV [25], $d_{\mathrm{C\text{-}C}} \sim 1.42$ Å and $\omega_R' \sim 224\ \mathrm{cm}^{-1} \cdot \mathrm{nm}/d'$ it follows from Eqs. (2), (4), and (5) that $\omega_R' - \omega_R \sim 40\ \mathrm{cm}^{-1}$ for semiconducting tubes, and $\sim 4\ \mathrm{cm}^{-1}$ for metallic tubes. Furthermore, for fixed laser frequency, we see that the laser couples preferentially to isolated tubes with diameter d' and bundled tubes with diameter d, where $\Delta d = d' - d \cong -0.2d^2/\alpha$. Regardless of the tube type (semiconducting or metallic), the net result of debundling is an apparent up-shift in the Raman active radial breathing mode frequency for the S-SWNTs using the same excitation frequency. Recently, Duesberg *et al.* [26] found using the 633 nm excitation that ω_R up-shifts from $\sim 188\ \mathrm{cm}^{-1}$ in a ~ 5 nm thick SWNT bundle to $\sim 193\ \mathrm{cm}^{-1}$ in a ~ 1.5 nm bundle.

Finally, it should be mentioned that the above explanation for the observed up-shift in the radial mode frequency assumes that α remains unchanged as bundled tubes are debundled [cf. Eqs. (3a) and (3b)]. An independent study based on LDA calculations will be necessary to verify the assumption made for α in this study.

A. M. R. and R. C. H. acknowledge financial support from the NSF MRSEC Grant No. 9809686, and P. C. E. through the NSF MRSEC Grant No. 9809686 and ONR Grant No. N00014-99-1-0619. U. D. V. acknowledges partial support of this research by the Donors of The Petroleum Research Fund, administered by the American Chemical Society. Y. K. K. and D. T. acknowledge financial support by the Office of Naval Research and DARPA under Grant No. N00014-99-1-0252.

*Author to whom correspondence should be addressed. Electronic address: arao@clemson.edu
†Present address: Zyvex Corporation, Richardson, TX 75081.
‡Present address: Department of Physics, University of California–Berkeley, Berkeley, CA 94720.

[1] A. M. Rao *et al.,* Science **275**, 187 (1997).
[2] A. Kasuya *et al.,* Phys. Rev. Lett. **78**, 4434 (1998).
[3] S. Bandow *et al.,* Phys. Rev. Lett. **80**, 3779 (1998).
[4] A. G. Rinzler *et al.,* Appl. Phys. A, Mater. Sci. Process. **67**, 29–37 (1998).
[5] J. Chen *et al.,* Science **282**, 95 (1998); J. Phys. Chem. B **105**, 2525 (2001).
[6] A. Thess *et al.,* Science **273**, 483 (1996).
[7] C. Journet *et al.,* Nature (London) **388**, 756 (1997).
[8] U. D. Venkateswaran *et al.,* Phys. Rev. B **59**, 10 928 (1999).
[9] E. Richter and P. C. Eklund (unpublished).
[10] D. Kahn and J. P. Lu, Phys. Rev. B **60**, 6535 (1999).
[11] L. Henrard *et al.,* Phys. Rev. B **60**, R8521 (1999).
[12] J. Kurti *et al.,* Phys. Rev. B **58**, R8869 (1998).
[13] P. Delany *et al.,* Nature (London) **391**, 466 (1998).
[14] Y. K. Kwon *et al.,* Phys. Rev. B **58**, R13 314 (1998).
[15] L. Alvarez *et al.,* Chem. Phys. Lett. **316**, 186 (2000).
[16] R. Saito, G. Dresselhaus, and M. S. Dresselhaus, *Physical Properties of Carbon Nanotubes* (Imperial College Press, London, 1998).
[17] A. M. Rao *et al.,* Nature (London) **388**, 257 (1997).
[18] M. Pimenta *et al.,* Phys. Rev. B **58**, R16 016 (1998). Note: In Ref. [18], the line shape of the tangential band is observed to be sensitive to the excitation laser energies. It was concluded in Ref. [18] that the laser energies in the interval 1.7–2.2 eV predominantly excite metallic SWNTs in the sample.
[19] D. Tománek and Michael A. Schluter, Phys. Rev. Lett. **67**, 2331 (1991).
[20] S. Sanvito, Y.-K. Kwon, D. Tománek, and C. J. Lambert, Phys. Rev. Lett. **84**, 1974 (2000).
[21] Y.-K. Kwon and D. Tománek, Phys. Rev. B **58**, R16 001 (1998).
[22] J. W. G. Wildoer *et al.,* Nature (London) **391**, 59 (1998).
[23] T. W. Odom, J. L. Huang, P. Kim, and C. M. Lieber, Nature (London) **391**, 62 (1998).
[24] H. Kataura *et al.,* Synth. Met. **103**, 2555 (1999).
[25] G. Dresselhaus *et al.,* in *Science and Applications of Nanotubes,* edited by D. Tománek and R. J. Enbody (Kluwer Academic, New York, 2000), pp. 275–295.
[26] G. S. Duesberg *et al.,* Phys. Rev. Lett. **85**, 5436 (2000).